

Structural Diversity and Luminescent Properties of the 2,2- and 2,3-Dimethylsuccinate Hybrid Lanthanide Frameworks

Supporting Information

Paul J. Saines,^a Mark Steinmann,^a Jin-Chong Tan,^{a,b} Hamish H.-M.
Yeung,^a and Anthony K. Cheetham*^a

^a*Department of Materials Science and Metallurgy, The University of Cambridge, Cambridge
CB2 3QZ, United Kingdom. Fax: +44 1223 334567; Tel: +44 1223 767061; E-mail:
akc30@cam.ac.uk*

^b*Department of Engineering Science, University of Oxford, Parks Rd., Oxford OX1 3PJ,
United Kingdom*

Synthetic Conditions

Framework **1**, $\text{La}(\text{C}_6\text{H}_8\text{O}_4)(\text{C}_6\text{H}_9\text{O}_4)(\text{H}_2\text{O})_2$, forms as colourless needle crystals and can be made with high purity at 100 °C from 0.6 mmol of $\text{LaCl}_3 \cdot 7\text{H}_2\text{O}$, 0.5 mmol of 2,2-DMS and 1.6 mmol of KOH in 9 mL of water, the quantity of solvent used throughout this study. Framework **2**, $\text{Ce}(\text{C}_6\text{H}_8.5\text{O}_4)_2(\text{H}_2\text{O})_2$, forms as colourless plate-like crystals at 100 °C using 1.3 mmol of $\text{CeCl}_3 \cdot 7\text{H}_2\text{O}$, 1.9 mmol of 2,2-DMS and 3.1 mmol of KOH. Using half the concentration of the reagents at 90 °C yields compound **3**, $\text{Ce}_2(\text{C}_6\text{H}_8\text{O}_4)_3(\text{H}_2\text{O})_2$, although the crystal used for structure determination was synthesized at 100 °C. Compounds **4** and **5**, $\text{Eu}_2(\text{C}_6\text{H}_8\text{O}_4)_3(\text{H}_2\text{O})_3$ and $\text{Tb}_2(\text{C}_6\text{H}_8\text{O}_4)_3(\text{H}_2\text{O})_3$, can be made in pure form at 100 °C and 150 °C, respectively, using 0.6 mmol of $\text{EuCl}_3 \cdot 6\text{H}_2\text{O}$ or $\text{TbCl}_3 \cdot 6\text{H}_2\text{O}$, 1.0 mmol of 2,2-DMS and 1.6 mmol of KOH, although the crystals used for the structural determination of the former were synthesized at 200 °C. Compound **4** often forms with small amounts of a Eu analogue of compound **3**.

Framework **6**, $\text{Y}_2(\text{C}_6\text{H}_8\text{O}_4)_3(\text{H}_2\text{O})_4 \cdot \text{H}_2\text{O}$ forms in pure form as colourless needles at 150 °C, using 0.6 mmol of $\text{YCl}_3 \cdot 6\text{H}_2\text{O}$, 1.0 mmol of 2,2-DMS and 1.6 mmol of KOH. At higher concentrations **6** forms along with compounds **7**, $\text{Y}_2(\text{C}_6\text{H}_8\text{O}_4)_3(\text{H}_2\text{O})_4$, or **8**, $\text{Y}_4(\text{C}_6\text{H}_8\text{O}_4)_6(\text{H}_2\text{O})$, using 2.5 mmol of $\text{YCl}_3 \cdot 6\text{H}_2\text{O}$, 3.8 mmol 2,2-DMS and 6.2 mmol KOH with crystals suitable for structure determination obtained at 100 °C and 200 °C, respectively. Compound **9**, which is isostructural with framework **7**, forms in high purity at 150 °C when 0.6 mmol of $\text{LuCl}_3 \cdot 6\text{H}_2\text{O}$, 1.0 mmol of 2,2-DMS and 1.6 mmol of KOH are used. Heating at 180 °C using the same starting materials yields a two phase mixture of compounds **10**, $\text{Lu}_2(\text{C}_6\text{H}_8\text{O}_4)_3(\text{H}_2\text{O})$ and **11**, $\text{Lu}_3(\text{C}_6\text{H}_8\text{O}_4)_4(\text{OH})(\text{H}_2\text{O})_2$ and at 200 °C, framework **11** forms in conjunction with **12**, $\text{Lu}_3(\text{C}_6\text{H}_8\text{O}_4)_4(\text{OH})$. Compound **13**, $\text{La}_2(\text{C}_6\text{H}_8\text{O}_4)_3(\text{H}_2\text{O})_2$, can be made between 150 °C and 200 °C, using 1.3 mmol of $\text{LaCl}_3 \cdot 7\text{H}_2\text{O}$, 1.9 mmol of a mixture of D-, L- and *meso*-isomers of 2,3-DMS and 3.1 mmol of KOH and can also be synthesized utilizing pure *meso*-2,3-DMS at 200 °C. Compound **14**, $\text{Y}_2(\text{C}_6\text{H}_8\text{O}_4)_3$, can be made at 200 °C using a similar concentration of reagents but substituting $\text{YCl}_3 \cdot 6\text{H}_2\text{O}$ for $\text{LaCl}_3 \cdot 7\text{H}_2\text{O}$ with either the mixture of 2,3-DMS isomers or the pure *meso*-form. The architectures described here are the only ones encountered during this study except for a $P\bar{1}$ triclinic phase that forms when reactions are carried out at 200 °C with La, which has a unit cell of $a = 12.2556(3)$ Å, $b = 18.9339(6)$ Å, $c = 25.9025(8)$ Å, $\alpha = 84.968(2)^\circ$, $\beta = 88.045(2)^\circ$ and $\gamma = 73.889(2)^\circ$ but whose structure was not possible to solve.

Ce, Eu and Tb doping of compounds **1**, **6** and **9** was carried out by substituting the appropriate percentage of the metal chloride source used for those of the host cations of a particular phase and using a total of 0.6 mmol of the metal chloride source, 1.0 mmol of 2,2-DMS and 1.6 mmol of KOH. The reaction temperature used was selected such that it gave single phase samples at 3 % doping levels. Consequently the doped samples of compound **1** were all made at 100 °C along with the Tb doped Y phases, while the Ce and Eu doped Y

phases were synthesized at 70 °C and 150 °C and all doped samples of phase **9** were made at 150 °C.

Single Crystal X-ray Structure Determinations

Table S1 Crystallographic Data for structures **1-5** determined by single crystal X-ray diffraction.

Compound	1	2	3	4	5
Formula	LaC ₁₂ H ₂₁ O ₁₀	CeC ₁₂ H ₂₁ O ₁₀	Ce ₂ C ₁₈ H ₂₈ O ₁₄	Eu ₂ C ₁₈ H ₃₀ O ₁₅	Tb ₂ C ₁₈ H ₃₀ O ₁₅
Formula Weight	463.50	465.41	748.64	790.36	804.26
T (K)	293(2)	120(2)	120(2)	120(2)	120(2)
Crystal System	Monoclinic	Orthorhombic	Triclinic	Orthorhombic	Orthorhombic
Space Group	<i>P2₁/c</i> (14)	<i>Pbcn</i> (60)	<i>P</i> $\bar{1}$ (2)	<i>Pccn</i> (56)	<i>Pccn</i> (56)
<i>a</i> (Å)	20.810(2)	20.7047(4)	11.0074(13)	34.7924(19)	34.6706(11)
<i>b</i> (Å)	8.8755(10)	8.86430(10)	11.1582(12)	12.5064(8)	12.5002(3)
<i>c</i> (Å)	8.9926(9)	8.89110(10)	12.1118(12)	11.5839(7)	11.5584(4)
α (°)	90	90	98.660(9)	90	90
β (°)	96.024(10)	90	103.678(9)	90	90
γ (°)	90	90	118.293(11)	90	90
V (Å ³)	1651.7(3)	1631.81(4)	1211.3(2)	5040.5(5)	5009.3(3)
Z	4	4	2	8	8
ρ_{calc} (g cm ⁻³)	1.864	1.894	2.053	2.083	2.133
μ (cm ⁻¹)	2.66	2.816	29.554	36.199	5.669
Refl. Meas./Unique	4454/4454 [Unmerged twin data]	15888/2812 [R _{int} = 0.0396]	8760/4593 [R _{int} = 0.0554]	11328/4824 [R _{int} = 0.0470]	18173/7617 [R _{int} = 0.0273]
Parameters Refined	104	114	325	325	340
R1, wR2 ^a (all)	0.0868, 0.1093	0.0359, 0.0516	0.0651, 0.1545	0.0591, 0.1260	0.0430, 0.0589
R1, wR2 ^a (obs)	0.0453, 0.0979	0.0227, 0.0456	0.0538, 0.1422	0.0510, 0.1205	0.0322, 0.0562
χ^2	1.001	1.047	1.073	1.073	1.161

$$^a \quad w = 1 / \left[\sigma^2 (F_o^2) + (aP)^2 + bP \right] \quad \text{and} \quad P = (\max(F_o^2, 0) + 2F_c^2) / 3; \quad R1 = \sum ||F_o| - |F_c|| / \sum |F_o| \quad \text{and}$$
$$wR2 = \sqrt{\left\{ \sum \left[w(F_o^2 - F_c^2)^2 \right] / \sum w(F_o^2)^2 \right\}}$$

Single crystal X-ray diffraction data of all compounds were obtained using an Oxford Diffraction Gemini Ultra diffractometer using MoK α radiation for compounds **1**, **2**, **5**, **6**, and **8-13** and CuK α for **3**, **4**, **7** and **14**. This instrument was equipped with an Eos CCD detector and the crystals were mounted on a cryoloop. Absorption corrections were carried out using analytical methods implemented in the program CrysAlis Pro¹ for the majority of compounds, although empirical multi-scan methods were used for **1** and **12** and gaussian methods for **7**, to compensate for the length of the needle shaped crystal using being larger than the size of the beam. Structures **1**, **5**, **13** and **14** were solved by Patterson synthesis using DIRDIF 2008² while direct methods, as implemented in SHELX-97³, were used for compounds **2-4** and **6-12**. All subsequent refinements were carried out against $|F|^2$ using SHELX-97³ via the Win-GX interface (see Table S1 and S2 for summary of crystal data).⁴ Attempts were made to solve the structure of **14** in space groups consistent with the observed systematic absences and to investigate the possibility of merohedral twinning but neither of these resulted in an improved model, either with regards to improved residual factors or the elimination of the extensive ligand disorder. The displacement parameters of all non-hydrogen atoms are refined anisotropically in most structures, although the parameter of the disordered atoms of the same type in structures **6**, **11** and **14** are constrained to be equal and, in the case of the pore water in **6** and all those in **14**, these were restrained to be approximately isotropic. The displacement parameters of C3 and C6 in **3** are restrained to be similar. The twinning in the crystal used to determine the structure of **1** and the relatively high complexity of the structure of **12**, combined with the presence of heavy lanthanide cations, led to unreasonable displacement parameters, often non-positive definite, when those of the non-lanthanide atoms were refined anisotropically and they were therefore only refined isotropically. The extensive disorder of the ligands in **14** required several of the bonds between the methyl carbon and the respective backbones to which they were attached be loosely restrained to a typical sp^3 C-C distance, chosen as 1.54 Å. While none of the restraints placed on the fitting to **14** significantly affected the residual factors the extensive disorder in this structure and the need for significant restraints means the details of this structure must be interpreted carefully although its connectivity is clear. The positions of the hydrogen atoms attached to the dicarboxylate ligands were geometrically constrained using the AFIX commands in SHELX-97.³ Where possible the aquo and hydroxyl hydrogen atoms were located from the Fourier difference map and were restrained to have a bond distance of 0.85 Å to the oxygen atoms to which they are attached, as well as constraining the intermolecular bond angles of water to an appropriate value. In the case of the water molecules in **1** and **4** and the disordered pore water in **6** this was not possible so AFIX commands in SHELX-97³ were utilized for **1** and **4** and they were omitted from the model of **6**. The displacement parameters of the hydrogen

atoms on the backbone of the ligand were constrained to be 1.2 times the size of the carbon to which they were attached, while those bonded to a methyl carbon or oxygen were fixed to be 1.5 times the atom to which they are bonded.

Table S2 Crystallographic Data for structures **6-8** and **10** determined by single crystal X-ray diffraction.

Compound	6	7	8	10
Formula	Y ₂ C ₁₈ H ₃₄ O ₁₇	YC ₉ H ₁₆ O ₈	Y ₄ C ₃₆ H ₅₀ O ₂₅	Lu ₂ C ₁₈ H ₂₆ O ₁₃
Formula Weight	700.265	341.13	1238.40	800.33
T (K)	120(2)	293(2)	293(2)	120(2)
Crystal System	Monoclinic	Triclinic	Triclinic	Monoclinic
Space Group	<i>P2₁/c</i> (13)	<i>P</i> $\bar{1}$ (2)	<i>P</i> $\bar{1}$ (2)	<i>P2₁/c</i> (14)
<i>a</i> (Å)	5.8422(3)	5.8717(8)	11.1645(5)	11.1375(4)
<i>b</i> (Å)	9.8906(4)	9.8057(18)	11.7892(10)	18.0442(5)
<i>c</i> (Å)	21.5267(10)	11.979(2)	18.3088(14)	12.7462(4)
α (°)	90	70.102(16)	89.219(6)	90
β (°)	93.957(4)	80.008(13)	87.563(5)	112.496(4)
γ (°)	90	89.723(13)	72.844(6)	90
V (Å ³)	1240.91(10)	637.60(18)	2300.5(3)	2366.65(13)
Z	2	2	2	4
ρ_{calc} (g cm ⁻³)	1.871	1.781	1.788	2.246
μ (cm ⁻¹)	7.003	6.822	5.082	8.347
Refl. Meas./Unique	4302/2353 [R _{int} = 0.0331]	3766/2368 [R _{int} = 0.0537]	16545/10285 [R _{int} = 0.0343]	10826/5425 [R _{int} = 0.0355]
Parameters Refined	168	188	604	310
R1, wR2 ^a (all)	0.0891, 0.1918	0.0759, 0.1951	0.0633, 0.0814	0.0392, 0.0663
R1, wR2 ^a (obs)	0.0860, 0.1903	0.0645, 0.1865	0.0321, 0.0627	0.0308, 0.0622
χ^2	1.241	1.147	0.966	1.039

Table S3 Crystallographic Data for structures **11-14** determined by single crystal X-ray diffraction.

Compound	11	12	13	14
Formula	Lu ₃ C ₂₄ H ₃₇ O ₁₉	Lu ₃ C ₂₄ H ₃₃ O ₁₇	LaC ₉ H ₁₄ O ₇	Y ₂ C ₁₈ H ₂₄ O ₁₂
Formula Weight	1154.211	1118.42	373.11	610.19
T (K)	120(2)	120(2)	120(2)	120(2)
Crystal System	Triclinic	Monoclinic	Monoclinic	Tetragonal
Space Group	<i>P</i> $\bar{1}$ (2)	<i>P</i> 2 ₁ / <i>c</i> (14)	<i>C</i> 2/ <i>c</i> (15)	<i>P</i> 4 ₁ 2 ₁ 2 (92)
<i>a</i> (Å)	11.8632(2)	15.9284(6)	22.7053(11)	17.6673(4)
<i>b</i> (Å)	13.0361(3)	16.2700(4)	12.3557(5)	17.6673(4)
<i>c</i> (Å)	13.1531(2)	11.8820(4)	8.3931(3)	15.1787(6)
α (°)	116.813(2)	90	90	90
β (°)	94.0420(10)	92.683(3)	93.878(4)	90
γ (°)	113.589(2)	90	90	90
V (Å ³)	1583.45(5)	3075.89(16)	2349.21(17)	4737.8(2)
Z	2	4	8	8
ρ_{calc} (g cm ⁻³)	2.421	2.413	2.11	1.711
μ (cm ⁻¹)	9.328	9.637	3.653	7.105
Refl.	79702/10907	14322/7065	5287/2699	9348/4554
Meas./Unique	[R _{int} = 0.0506]	[R _{int} = 0.0398]	[R _{int} = 0.0296]	[R _{int} = 0.0263]
Parameters Refined	441	203	177	395
R1, wR2 ^a (all)	0.0248, 0.0644	0.0550, 0.0692	0.0429, 0.0658	0.0416, 0.0985
R1, wR2 ^a (obs)	0.0236, 0.0634	0.0372, 0.0628	0.0308, 0.0604	0.0393, 0.0971
χ^2	1.114	1.037	1.003	1.075

Table S4 Cation coordination bond distances in frameworks **1-5** (Å). * has been used to note multiple bonds between pairs of crystallographically identical atoms.

	1		3		Ce2-O12	2.620(7)		5
La1-O12*	2.522(10)	Ce1-O2	2.441(9)	4	Tb1-O1	2.280(3)		
La1-O13	2.544(9)	Ce1-O13*	2.444(6)	Eu1-O1	2.303(5)	Tb1-O11	2.346(3)	
La1-O1W	2.568(6)	Ce1-O24	2.456(7)	Eu1-O11	2.364(6)	Tb1-O2W	2.356(4)	
La1-O2*	2.568(8)	Ce1-O2W	2.510(6)	Eu1-O2W	2.382(6)	Tb1-O21	2.375(3)	
La1-O2W	2.582(8)	Ce1-O1W	2.536(8)	Eu1-O21	2.389(5)	Tb1-O22	2.400(2)	
La1-O1	2.583(7)	Ce1-O13*	2.558(7)	Eu1-O22	2.404(6)	Tb1-O23	2.411(3)	
La1-O4	2.636(9)	Ce1-O14	2.579(6)	Eu1-O1W	2.437(5)	Tb1-O1W	2.418(3)	
La1-O12*	2.663(9)	Ce1-O12	2.608(7)	Eu1-O23	2.444(5)	Tb1-O24	2.514(2)	
La1-O2*	2.695(7)	Ce1-O1	2.624(7)	Eu1-O24	2.516(5)	Tb2-O12	2.244(3)	
La1-O11	2.715(7)	Ce2-O11	2.423(8)	Eu2-O12	2.266(5)	Tb2-O2	2.268(3)	
2		Ce2-O3*	2.435(7)	Eu2-O2	2.283(5)	Tb2-O13*	2.373(3)	
Ce1-O4	2 × 2.5147(14)	Ce2-O21	2.522(7)	Eu2-O13*	2.387(5)	Tb2-O3W	2.376(3)	
Ce1-O1W	2 × 2.5418(15)	Ce2-O22	2.546(6)	Eu2-O3W	2.402(6)	Tb2-O4	2.409(2)	
Ce1-O2	2 × 2.5813(14)	Ce2-O1W	2.548(7)	Eu2-O4	2.433(5)	Tb2-O14	2.441(3)	
Ce1-O3	2 × 2.6166(16)	Ce2-O3*	2.552(6)	Eu2-O14	2.463(6)	Tb2-O13*	2.493(2)	
Ce1-O4	2 × 2.6493(14)	Ce2-O4	2.555(8)	Eu2-O3	2.512(5)	Tb2-O3	2.498(2)	
		Ce2-O1	2.567(8)	Eu2-O13*	2.516(5)			

Table S5 Cation coordination bond distances in frameworks **6-10** (Å). * has been used to note multiple bonds between pairs of crystallographically identical atoms.

	6		8	Y3-O41	2.215(3)	Lu1-O11	2.507(9)
Y1-O1	2.208(6)	Y1-O13*	2.266(2)	Y3-O54	2.249(2)	10	
Y1-O2	2.282(7)	Y1-O24	2.298(3)	Y3-O34	2.258(3)	Lu1-O23	2.195(3)
Y1-O2W	2.354(8)	Y1-O1	2.304(2)	Y3-O4	2.295(2)	Lu1-O11	2.238(5)
Y1-O1W	2.356(8)	Y1-O2	2.312(3)	Y4-O53	2.235(3)	Lu1-O1W	2.256(3)
Y1-O3	2.378(7)	Y1-O21	2.315(2)	Y4-O3	2.246(3)	Lu1-O14	2.288(3)
Y1-O12	2.395(7)	Y1-O14	2.407(2)	Y4-O42	2.247(3)	Lu1-O4	2.353(5)
Y1-O11	2.430(8)	Y1-O11	2.446(2)	Y4-O12	2.254(2)	Lu1-O1	2.382(3)
Y1-O4	2.441(7)	Y1-O13*	2.564(3)	Y4-O52	2.292(2)	Lu1-O2	2.388(3)
	7	Y2-O44	2.250(2)	Y4-O32	2.328(2)	Lu1-O3	2.443(5)
Y1-O4	2.234(7)	Y2-O23	2.317(3)	Y4-O31	2.547(2)	Lu2-O12	2.241(3)
Y1-O3	2.279(9)	Y-O33	2.325(2)	9		Lu2-O3	2.255(3)
Y1-O2W	2.350(9)	Y2-O1W	2.353(3)	Lu1-O4	2.226(9)	Lu2-O24	2.260(4)
Y1-O12	2.379(8)	Y2-O31	2.364(3)	Lu1-O3	2.244(11)	Lu2-O1	2.290(3)
Y1-O1W	2.381(9)	Y2-O22	2.404(2)	Lu1-O2W	2.269(10)	Lu2-O22	2.349(3)
Y1-O1	2.400(8)	Y2-O11	2.462(2)	Lu1-O12	2.343(8)	Lu2-O21	2.350(5)
Y1-O2	2.418(10)	Y2-O21	2.499(2)	Lu1-O1W	2.369(12)	Lu2-O13	2.360(3)
Y1-O11	2.452(7)	Y3-O43	2.916(2)	Lu1-O1	2.429(12)	Lu2-O14	2.468(4)
		Y3-O51	2.206(3)	Lu1-O2	2.481(12)		

Table S6 Cation coordination bond distances in frameworks **11-13** (Å). In **11** O11 is disordered over two sites with 50 % fractional occupancy. * has been used to note multiple bonds between pairs of crystallographically identical atoms.

	11	Lu3-O23	2.300(3)	Lu2-O3	2.463(4)
Lu1-O1H	2.193(3)	Lu3-O13	2.3553(17)	Lu3-O22	2.193(5)
Lu1-O1	2.214(3)	Lu3-O14	2.3897(16)	Lu3-O33	2.224(4)
Lu1-O33	2.230(2)	Lu3-O3	2.4395(19)	Lu3-O12	2.228(5)
Lu1-O11	2.265(7)	Lu3-O4	2.4529(16)	Lu3-O13	2.243(5)
Lu1-O11A	2.260(7)	12		Lu3-O34	2.259(5)
Lu1-O22	2.286(3)	Lu1-O23	2.150(5)	Lu3-O31	2.344(5)
Lu1-O1W	2.3320(19)	Lu1-O24	2.214(5)	Lu3-O1H	2.423(4)
Lu1-O2W	2.337(2)	Lu1-O1	2.236(4)	13	
Lu2-O1H	2.154(3)	Lu1-O3	2.259(4)	La1-O3	2.448(4)
Lu2-O12	2.223(3)	Lu1-O1H	2.285(4)	La1-O4	2.504(3)
Lu2-O34	2.225(16)	Lu1-O32	2.342(5)	La-O11	2.506(3)
Lu2-O31	2.237(3)	Lu1-O31	2.374(5)	La1-O12	2.527(3)
Lu2-O4	2.307(2)	Lu2-O14	2.157(5)	La1-O1*	2.542(3)
Lu2-O24	2.383(2)	Lu2-O21	2.193(4)	La1-O1W	2.564(3)
Lu2-O23	2.4813(17)	Lu2-O2	2.195(4)	La1-O2	2.608(3)
Lu3-O21	2.188(3)	Lu2-O11	2.230(5)	La1-O12	2.659(3)
Lu3-O2	2.221(3)	Lu2-O1H	2.336(4)	La1-O1*	2.723(3)
Lu3-O32	2.259(3)	Lu2-O4	2.374(5)		

Table S7 Microanalysis results from compounds **1-6, 9, 13** and **14**.

Compound	% C determined	% C calculated	% H determined	% H calculated
1	31.01	31.05	4.45	4.55
2	30.44	30.97	4.39	4.55
3	28.76	28.88	3.69	3.77
4	27.45	27.36	3.74	3.83
5	26.86	26.88	3.69	3.76
6	31.00	30.87	4.76	4.89
9	25.29	25.30	3.71	3.78
13	28.78	28.97	3.66	3.78
14	35.25	35.41	3.91	3.92

Table S8 Crystallographic details for compound **9**. The structure is triclinic $P\bar{1}$ with $a = 5.81285(6)$ Å, $b = 9.77420(8)$ Å, $c = 11.95638(18)$ Å, $\alpha = 70.0638(7)^\circ$, $\beta = 79.8209(9)^\circ$ and $\gamma = 89.4864(9)^\circ$. The displacement parameters (U) were refined isotropically and those of each type of atom were constrained to be the same; refining to $0.0114(4)$ Å², $0.029(3)$ Å² and $0.008(1)$ Å² for Lu, C and O respectively. The fractional occupancies of C13 and C14 are 0.5 and all other atomic sites are fully occupied.

Atom	x	y	z
Lu1	0.3740(2)	0.74996(13)	0.60735(11)
C1	0.1179(24)	0.7265(13)	0.4332(13)
C2	-0.0071(23)	0.7261(12)	0.3289(10)
C3	0.1151(17)	1.1336(10)	0.7435(8)
C4	-0.0856(21)	1.0345(14)	0.8353(10)
C5	0.2905(24)	1.1607(14)	0.8163(12)
C6	0.2336(23)	1.0591(11)	0.6558(10)
C11	0.0784(16)	0.5857(16)	0.8264(6)
C12	-0.0775(12)	0.5147(10)	0.9519(5)
C13	-0.175(4)	0.3672(18)	0.9561(17)
C14	-0.2710(30)	0.6154(23)	0.9760(21)
O1	0.1034(18)	0.8361(10)	0.4681(11)
O2	0.2577(17)	0.6277(9)	0.4733(9)
O3	0.2081(18)	0.9268(9)	0.6685(10)
O4	0.3893(18)	1.1258(11)	0.5656(10)
O11	-0.0013(18)	0.6133(10)	0.7303(6)
O12	0.2846(15)	0.6291(10)	0.8172(8)
O1W	0.6887(19)	0.8474(10)	0.6637(9)
O2W	0.6231(19)	0.5668(10)	0.6261(9)

Infrared Spectroscopy

Infra-red spectra were collected between 4000 cm^{-1} and 500 cm^{-1} on a Bruker Tensor-27 ATR spectrometer. The spectrum of **1** has absorption bands at: $\nu_{\text{max}}/\text{cm}^{-1}$ (likely assignment): 3550 and 3400 (OH broad); 2974, 2939 and 2873 (C-CH₃); 1743 (C=O from protonated dicarboxylate groups); 1643 and 1562 ($\nu_{\text{as}}\text{ CO}_2^-$); 1473, 1454 and 1404 ($\nu_{\text{s}}\text{ CO}_2^-$); 1299, 1257 and 1204 (CH₃ and C-O); 1157, 1130, 1060, 1029 ($\nu_{\text{as}}\text{ C-C}$) and 991, 952, 922, 875, 829,

791, 756, 675, 605, 571 and 540 (metal-oxygen bonding and C-H).⁵ The spectrum of **2** has absorption bands at: 3560 and 3400 (OH broad); 2974, 2932 and 2873 (C-CH₃); 1744 (C=O from protonated dicarboxylate groups); 1643, 1601 and 1562 ($\nu_{\text{as}} \text{CO}_2^-$); 1477, 1450 and 1411 ($\nu_{\text{s}} \text{CO}_2^-$); 1300, 1258 and 1204 (CH₃ and C-O); 1134, 1111 and 1030 ($\nu_{\text{as}} \text{C-C}$) and 991, 957, 926, 880, 829, 795, 756, 675, 606, 578 and 544 (metal-oxygen bonding and C-H).

The spectrum of **3** has absorption bands at: 3591, 3298, and 3229 (OH); 2970, 2928 and 2870 (C-CH₃); 1605, 1585, and 1542 ($\nu_{\text{as}} \text{CO}_2^-$); 1473, 1454 and 1400 ($\nu_{\text{s}} \text{CO}_2^-$); 1292, 1250, 1215 and 1191 (CH₃ and C-O); 1122, 1065 and 1022 ($\nu_{\text{as}} \text{C-C}$) and 988, 949, 899, 837, 787, 768, 683, 663, 579, 552 and 524 (metal-oxygen bonding and C-H). The spectrum of **4** has absorption bands at: 3533, 3330 and 3205 (OH); 2966, 2927 and 2870 (C-CH₃); 1630, 1600, 1555 and 1516 ($\nu_{\text{as}} \text{CO}_2^-$); 1474 and 1427 ($\nu_{\text{s}} \text{CO}_2^-$); 1377, 1361, 1300, 1261 and 1222 (CH₃ and C-O); 1165 and 1144 ($\nu_{\text{as}} \text{C-C}$) and 1018, 991, 957, 895, 845, 833, 787, 741, 636, 617, 590, 570 and 540 (metal-oxygen bonding and C-H). The spectrum of **5** has absorption bands at: 3529, 3330 and 3210 (OH); 2966, 2928 and 2870 (C-CH₃); 1635, 1604, 1555 and 1519 ($\nu_{\text{as}} \text{CO}_2^-$); 1474 and 1427 ($\nu_{\text{s}} \text{CO}_2^-$); 1377, 1362, 1300, 1261 and 1222 (CH₃ and C-O); 1165 and 1145 ($\nu_{\text{as}} \text{C-C}$) and 1018, 991, 960, 900, 848, 833, 790, 745, 667, 636, 618, 590, 567 and 540 (metal-oxygen bonding and C-H).

The spectrum of **6** has absorption bands at: 3510 and 3250 (OH broad); 2982, 2939 and 2878 (C-CH₃); 1670, 1640 and 1520 ($\nu_{\text{as}} \text{CO}_2^-$); 1477 and 1430 ($\nu_{\text{s}} \text{CO}_2^-$); 1377, 1292, 1265, 1227 and 1204 (CH₃ and C-O); 1173, 1161, 1142 and 1118 ($\nu_{\text{as}} \text{C-C}$) and 1022, 988, 945, 918, 899, 826, 787, 737, 705, 664, 636, 598 and 547 (metal-oxygen bonding and C-H). The spectrum of **9** has absorption bands at: 3500 and 3420 (OH broad); 3000, 2986, 2966 and 2932 (C-CH₃); 1678, 1639, 1589, and 1535 ($\nu_{\text{as}} \text{CO}_2^-$); 1477 and 1431 ($\nu_{\text{s}} \text{CO}_2^-$); 1396, 1362, 1296, 1269 and 1223 (CH₃ and C-O); 1161 ($\nu_{\text{as}} \text{C-C}$) and 1018, 995, 949, 922, 903, 784, 733, 671, 633, 600, 574 and 544 (metal-oxygen bonding and C-H).

The spectrum of compound **13** has bands at: 3314 (OH, broad); 2974, 2947 and 2885 (C-CH₃); 1531 ($\nu_{\text{as}} \text{CO}_2^-$); 1454 and 1416 ($\nu_{\text{s}} \text{CO}_2^-$) 1368, 1316, 1300, 1273 and 1216 (CH₂, CH₃ and C-O); 1165 and 1068 ($\nu_{\text{as}} \text{C-C}$) and 1007, 972, 930, 898, 826, 795, 764, 664 and 563 (metal-oxygen bonding and C-H). The spectrum of compound **14** has absorption bands at: 2974 and 2939 (C-CH₃); 1541 ($\nu_{\text{as}} \text{CO}_2^-$); 1465 and 1422 ($\nu_{\text{s}} \text{CO}_2^-$); 1362, 1300 and 1220 (CH₂, CH₃ and C-O); 1084 ($\nu_{\text{as}} \text{C-C}$); 976, 937, 907, 795, 745, 660, 582 and 563 (metal-oxygen bonding and C-H).

Thermal Analysis

The decomposition of compound **1** is particularly complex with several distinct temperature ranges over which weight is lost (see Fig. S21). Firstly its coordinated water molecules are lost between 100 °C and 150 °C (% of initial weight remaining 92.1 % c.f. to expected 92.2 %). Further weight loss occurs in two periods between 150 °C and 320 °C leading to 61.0 % weight remaining, corresponding to the further loss of one of its 2,2-DMS ligands (60.9 % expected). Yet higher temperatures lead to further weight loss corresponding to the decomposition of the remaining 2,2-DMS ligand with a final weight recorded at 800 °C of 34.9 %. This corresponds well with the formation of La_2O_3 (35.2 % expected), consistent with PXRD measurements of the TGA residue. The weight loss of **2** is similar but simpler than is the case for **1** with its coordinated water lost between 80 °C and 150 °C (observed and expected weight remaining of 92.1 % and 92.7 %). Further decline occurs in two periods between 150 °C and 340 °C, roughly consistent with complete decomposition to CeO_2 (observed weight at 340 °C was 38.1 % compared to an expected residual of 37.0 % for the formation of CeO_2), consistent with PXRD measurements (see Fig. S22 for TGA plot). Compound **3** loses 5.4 % of its weight between 150 °C and 230 °C, consistent with it losing the water in its structure at this temperature (weight change of 4.8 % expected; see Fig S23) before complete decomposition above 280 °C leads to an observed weight consistent with the formation of Ce_2O_3 at 400 °C (44.0 % observed remaining compared to 43.8 %). Subsequent weight gain occurs above 800 °C, suggestive of the oxidation of the decomposition product, most likely to CeO_2 .

Compounds **4** and **5** both lose their coordinated water molecules around 140-150 °C (observed and expected weight remaining at 260 °C of 93.2 % and 93.5 % for **4** and 93.3 % and 93.5 %, for **5**, respectively; see Fig S24 and S25). The remainder of both complexes decompose above 350 °C with **4** having a residue of 45.6 % at 670 °C consistent with decomposition to Eu_2O_3 , as indicated by PXRD (44.5 % expected). While the majority of weight loss from **5** following decomposition is complete by 550 °C there is continual gradual weight loss to 45.5 % at 950 °C, consistent with the formation of Tb_7O_{11} as indicated by PXRD (expected weight remaining of 46.3 %). **6** loses both its pore and coordinated water at a similar temperature to the one dimensional polymers, with this occurring between 110 °C and 170 °C (88.0 % weight remaining at the end of this period compared to 87.1 % expected; see Fig S26 for plot) with the framework completely decomposing between 350 °C and 425 °C, with gradual decrease in weight thereafter to 33.0 % at 790 °C. This is consistent with the formation of Y_2O_3 as observed in XRD (32.2 % weight remaining). **9** retains its water molecules to a slightly higher temperature than **6** (see Fig. S27), losing them between 130 °C and 210 °C (expected and observed weight change of 8.2 and 8.4 %). It then decomposes between 380 °C and 600 °C, possibly to $\text{La}(\text{OH})_3$ (observed and expected remaining weight of 52.9 and 51.3 %), before subsequent further decomposition to La_2O_3 , consistent with PXRD (observed and expected remaining weight of 46.8 and 46.6 %).

Compound **13** loses its water molecules above 110 °C with a weight change of 4.8 % recorded up to 230 °C, as expected. It then decomposes at 320 °C with gradual weight loss continuing to occur to 800 °C consistent with the ultimate formation of La_2O_3 (observed and expected weight remaining of 43.7 % and 44.4%; see Fig. S28). The decomposition of **14** is relatively simple, due to it being anhydrous, decomposing to Y_2O_3 above 360 °C, consistent with PXRD, leading to an observed weight of 36.7 % compared to an expected weight of 37.0 % (see Fig. S29).

Supplementary Figures

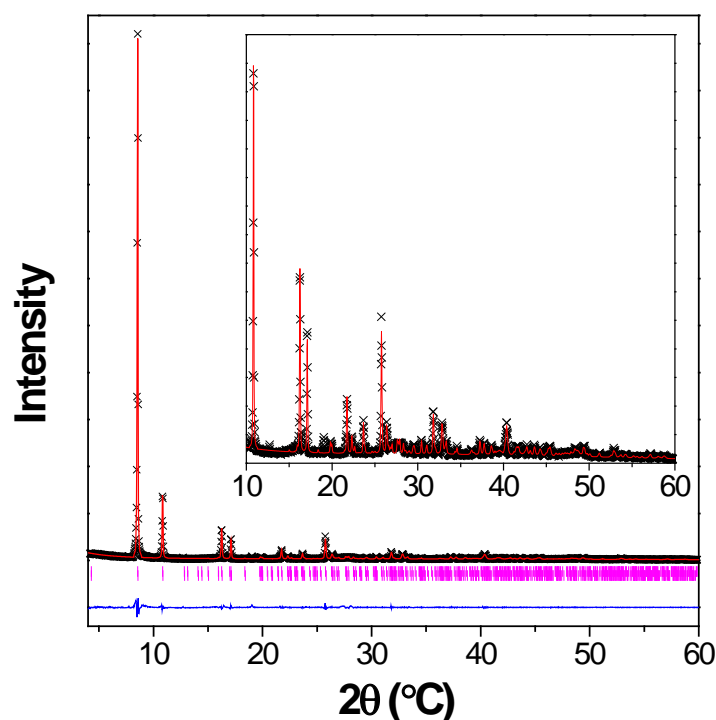


Fig. S1 Conventional (laboratory) X-ray diffraction pattern of **1** fitted using the Le Bail method in the program Rietica.⁶ The observed intensity, calculated intensity and difference plot are marked with black crosses and red and blue lines, respectively. The Bragg reflections are marked by magneta vertical markers and the insert shows the weaker reflections in greater detail. The unit cell refined as $a = 20.8585(14)$ Å, $b = 8.9021(6)$ Å, $c = 8.9699(11)$ Å and $\beta = 95.843(13)^\circ$. R_p , R_{wp} and χ^2 are 7.3 %, 11.0 % and 4.5.

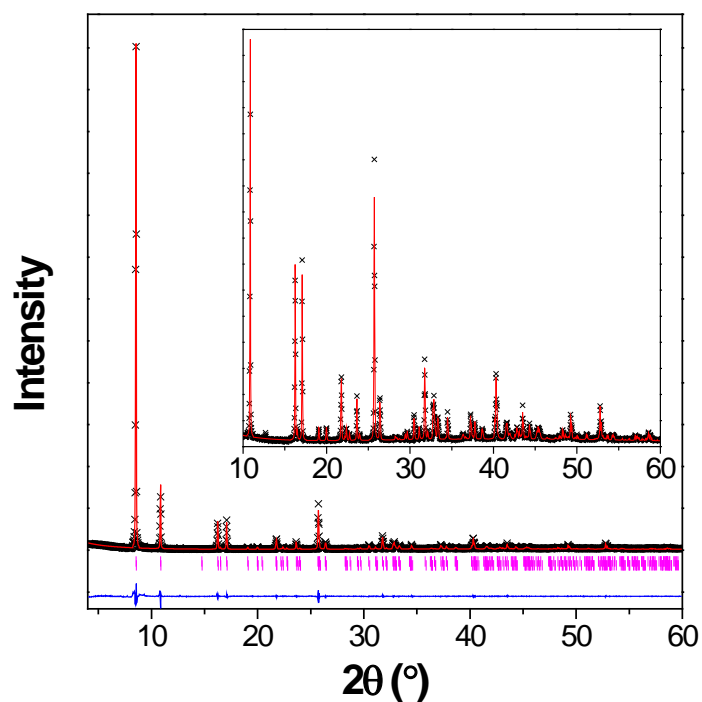


Fig. S2 Conventional X-ray diffraction pattern of **2** fitted using the Le Bail method in the program Rietica.⁶ The format is the same as Fig. S1. The unit cell refined as $a = 20.8125(5)$ Å, $b = 8.8954(3)$ Å and $c = 8.9152(6)$ Å. R_p , R_{wp} and χ^2 are 7.4 %, 11.1 % and 4.2.

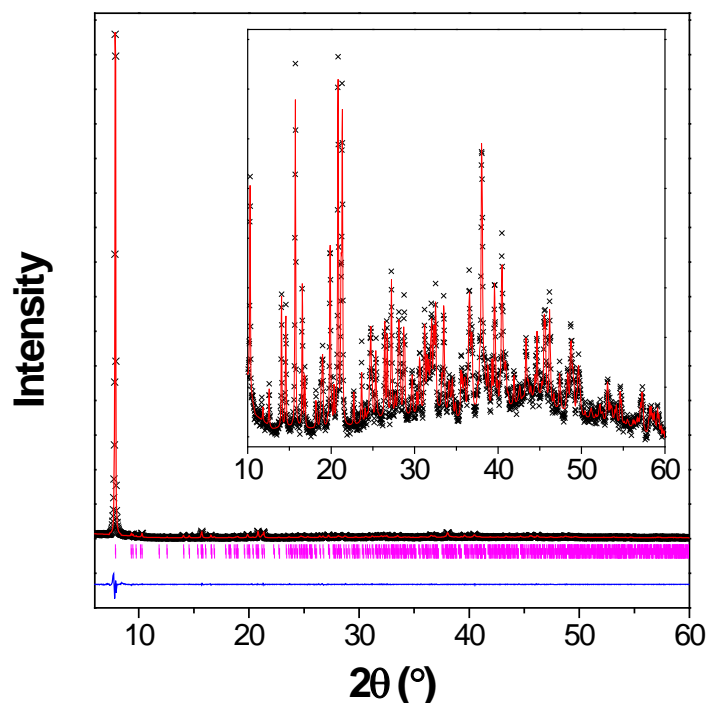


Fig. S3 Conventional X-ray diffraction pattern of **3** fitted using the Le Bail method, implemented in the program Rietica.⁶ The format is the same as Fig. S1. The unit cell refined as $a = 11.0170(8)$ Å, $b = 11.1614(7)$ Å, $c = 12.1414(15)$ Å, $\alpha = 98.654(7)^\circ$, $\beta = 103.662(7)^\circ$ and $\gamma = 118.324(6)^\circ$. R_p , R_{wp} and χ^2 are 5.0 %, 8.1 % and 5.4.

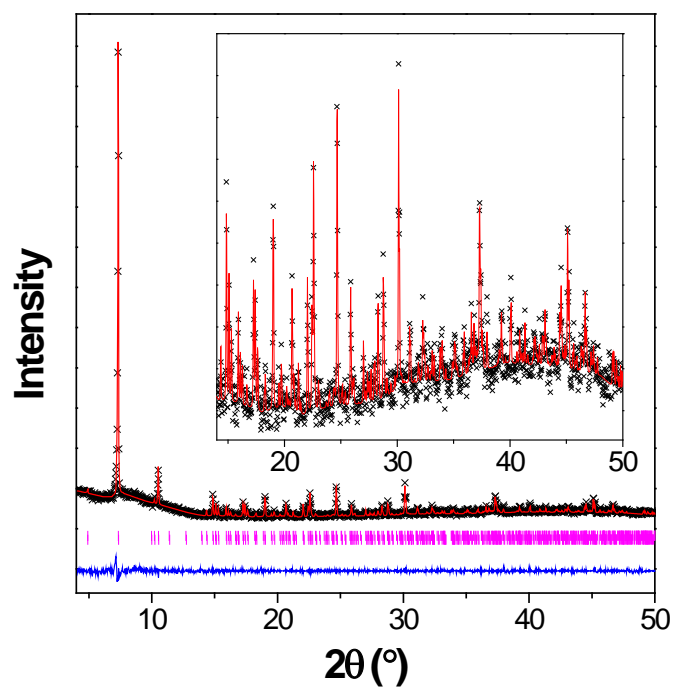


Fig. S4 Conventional X-ray diffraction pattern of **4** fitted using the Le Bail method, implemented in the program Rietica.⁶ The format is the same as Fig. S1. The unit cell refined as $a = 34.8890(15)$ Å, $b = 12.5359(8)$ Å and $c = 11.6145(8)$ Å. R_p , R_{wp} and χ^2 are 4.9 %, 6.4 % and 0.94.

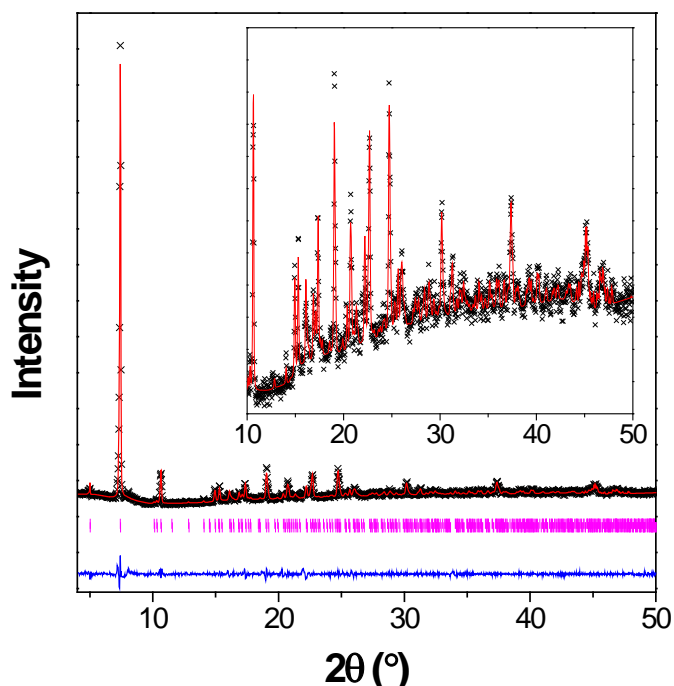


Fig. S5 Conventional X-ray diffraction pattern of **5** fitted using the Le Bail method, implemented in the program Rietica.⁶ The format is the same as Fig. S1. The unit cell refined as $a = 34.691(4)$ Å, $b = 12.5275(16)$ Å and $c = 11.5338(9)$ Å. R_p , R_{wp} and χ^2 are 3.9 %, 5.4 % and 1.9.

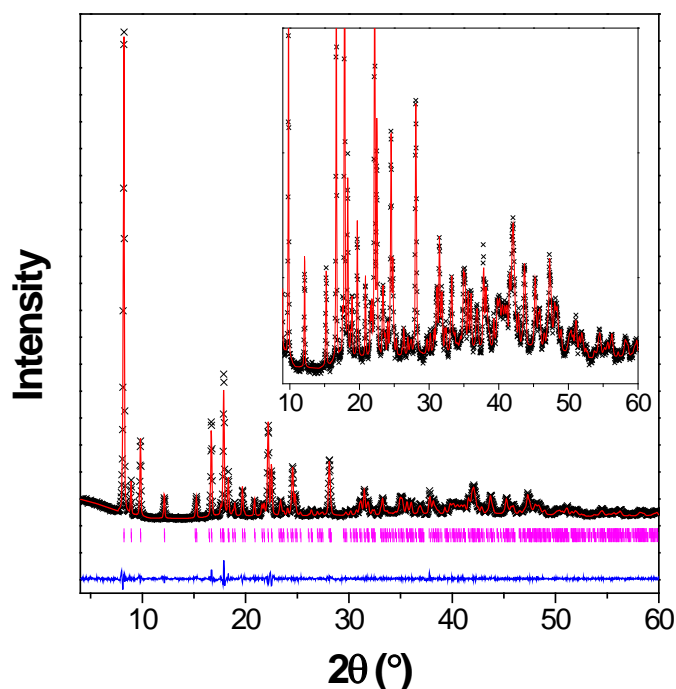


Fig. S6 Conventional X-ray diffraction pattern of **6** fitted using the Le Bail method, implemented in the program Rietica.⁶ The format is the same as Fig. S1. The unit cell refined as $a = 5.8745(2) \text{ \AA}$, $b = 9.9228(4) \text{ \AA}$, $c = 21.5876(12) \text{ \AA}$ and $\beta = 94.209(3)^\circ$. R_p , R_{wp} and χ^2 are 4.1 %, 5.6 % and 2.1.

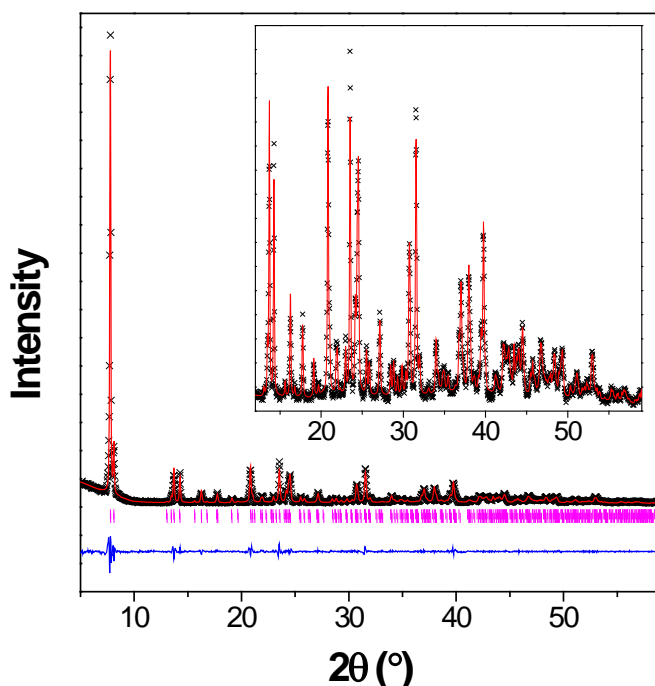


Fig. S7 Conventional X-ray diffraction pattern of **13** fitted using the Le Bail method, implemented in the program Rietica.⁶ The format is the same as Fig. S1. The unit cell refined as $a = 22.7158(13) \text{ \AA}$, $b = 12.4307(8) \text{ \AA}$, $c = 8.4742(7) \text{ \AA}$ and $\beta = 93.889(7)^\circ$. R_p , R_{wp} and χ^2 are 6.1 %, 8.3 % and 2.2.

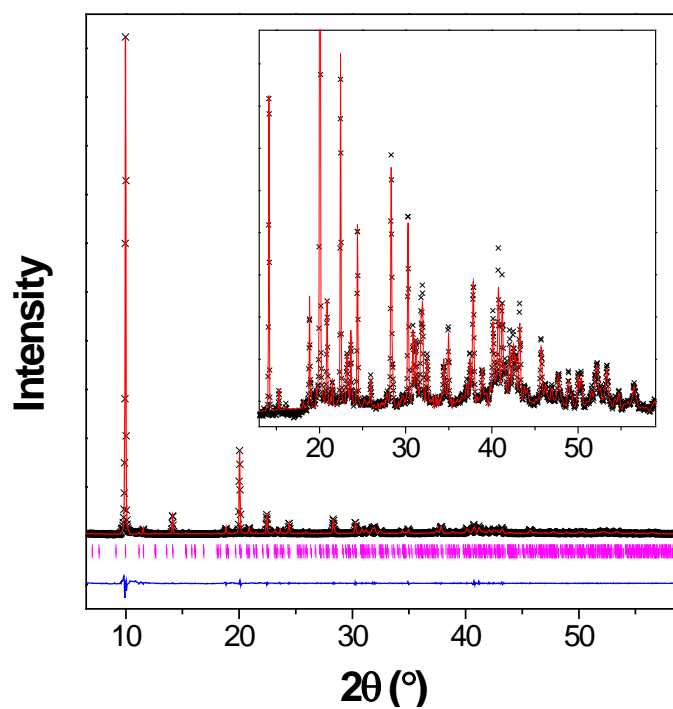


Fig. S8 Conventional X-ray diffraction pattern of **14** fitted using the Le Bail method, implemented in the program Rietica.⁶ The format is the same as Fig. S1. The unit cell refined as $a = 17.6699(7) \text{ \AA}$ and $c = 15.2002(9) \text{ \AA}$ while R_p , R_{wp} and χ^2 are 6.1 %, 10.2 % and 8.9.

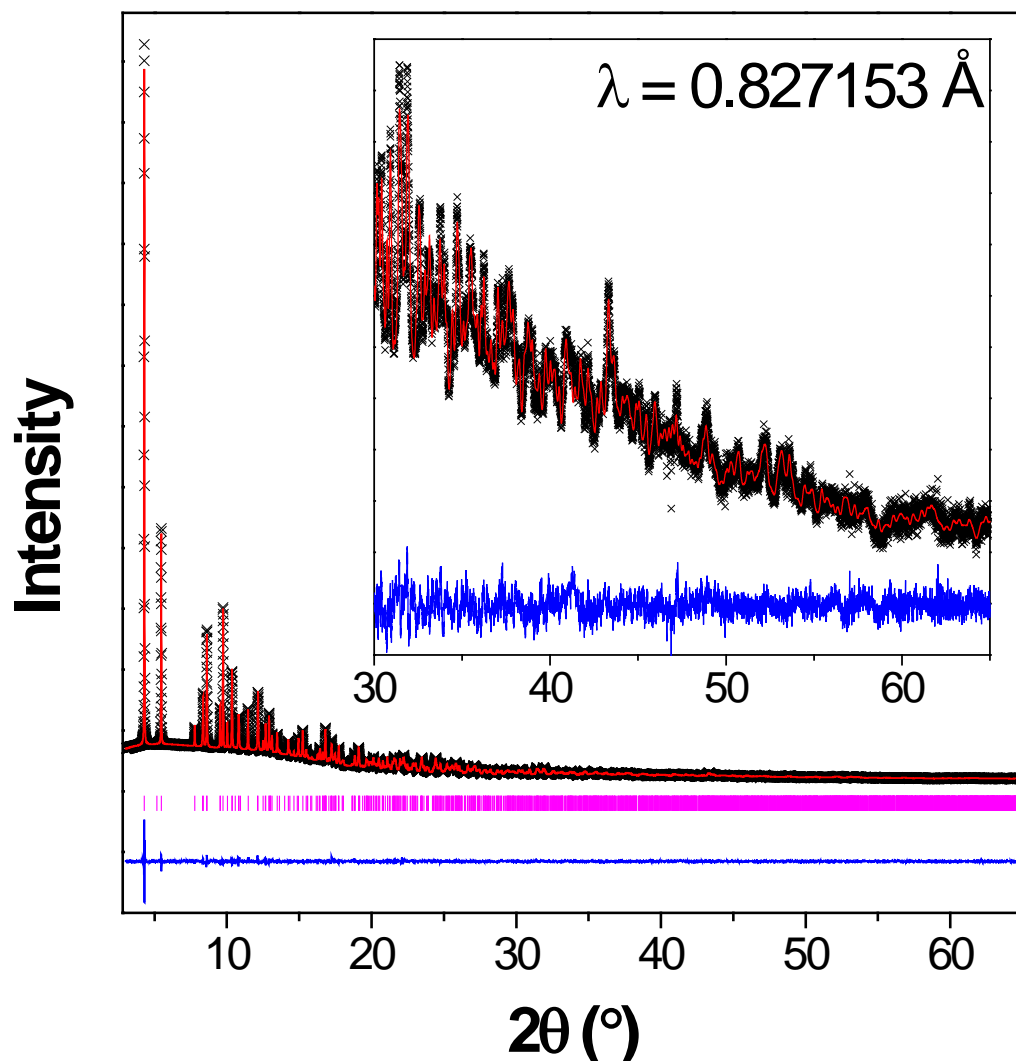


Fig. S9 Synchrotron X-ray diffraction pattern of **9** fitted using the Rietveld method. The format is the same as Fig. S1 and R_p , R_{wp} and χ^2 refined as 1.5 %, 2.1 % and 45.6.

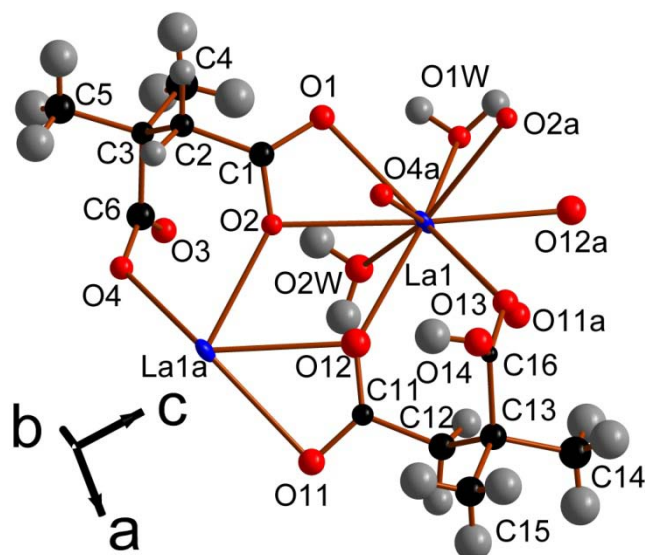


Fig. S10 The asymmetric unit of **1** with 40 % probability ellipsoids. The labels on the hydrogen atoms are omitted for the sake of clarity and additional non-hydrogen atoms, included to illustrate the coordination sphere of all cations and ligand atoms in the structure, are labelled alphabetically. The colours are the same as in Fig. 1.

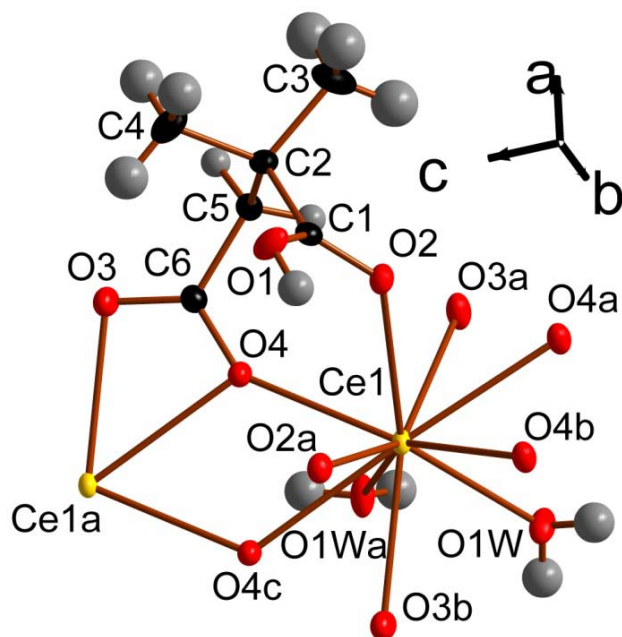


Fig. S11 The asymmetric unit of **2** with 60 % probability ellipsoids. The labels on the hydrogen atoms are omitted for the sake of clarity and additional non-hydrogen atoms, included to illustrate the coordination sphere of all cations and ligand atoms in the structure, are labelled alphabetically. The colours are the same as in Fig. 2.

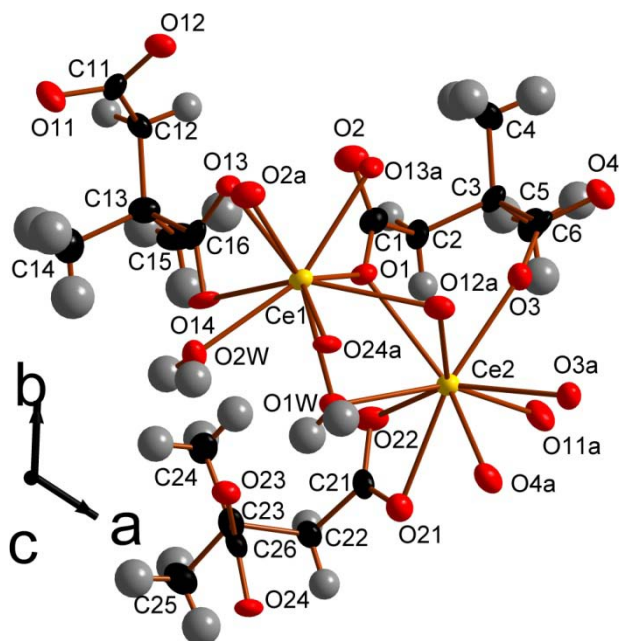


Fig. S12 The asymmetric unit of **3** with 60 % probability ellipsoids. The labels on the hydrogen atoms are omitted for the sake of clarity and additional non-hydrogen atoms, included to illustrate the coordination sphere of all cations in the structure, are labelled alphabetically. The colours are the same as in Fig. 2.

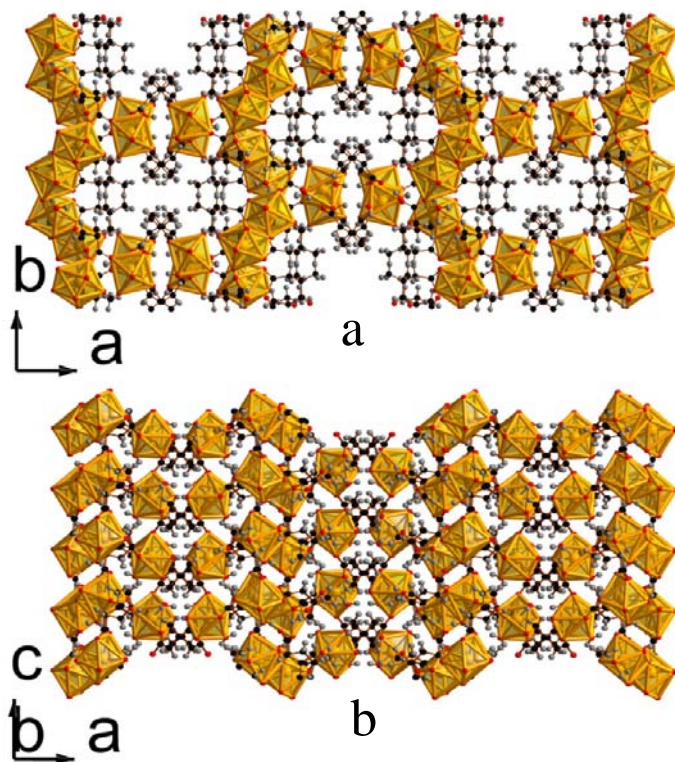


Fig. S13 The structure of compound **4** showing the a) *ab* and b) *ac* planes. The colours are as in Fig. 2.

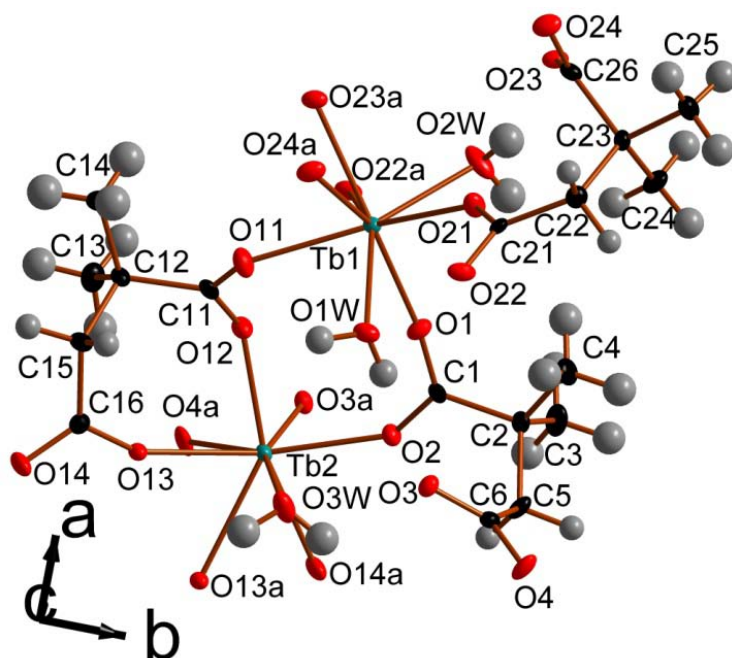


Fig. S14 The asymmetric unit of **5** with 60 % probability ellipsoids. The labels on the hydrogen atoms are omitted for the sake of clarity and additional non-hydrogen atoms, included to illustrate the coordination sphere of all cations in the structure, are labelled alphabetically. The colours are the same as in Fig. 4.

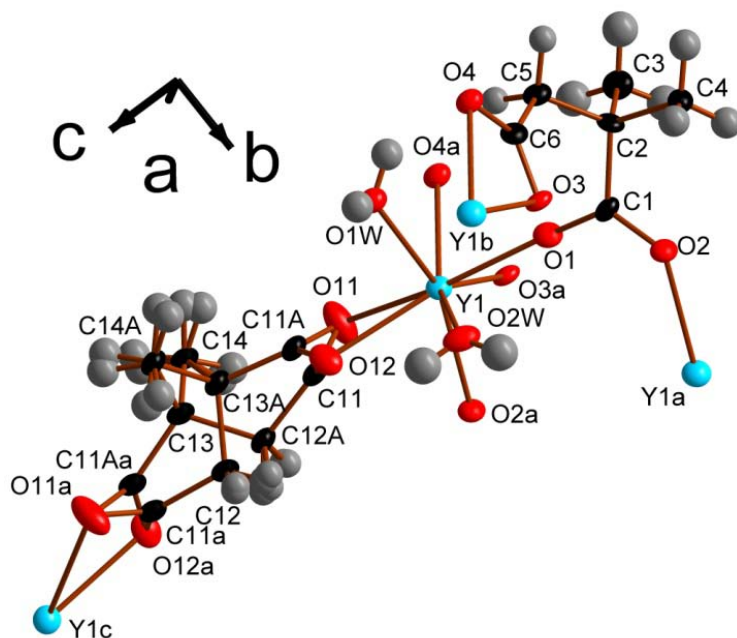


Fig. S15 The asymmetric unit of **6** with 40 % probability ellipsoids. The labels on the hydrogen atoms are omitted for the sake of clarity. Additional non-hydrogen atoms, illustrating the coordination sphere of all cations and oxygen atoms are labelled alphabetically. Both components of the disordered ligand are displayed and the colours are the same as in Fig. 5. The disordered oxygen atoms from pore water molecules are omitted.

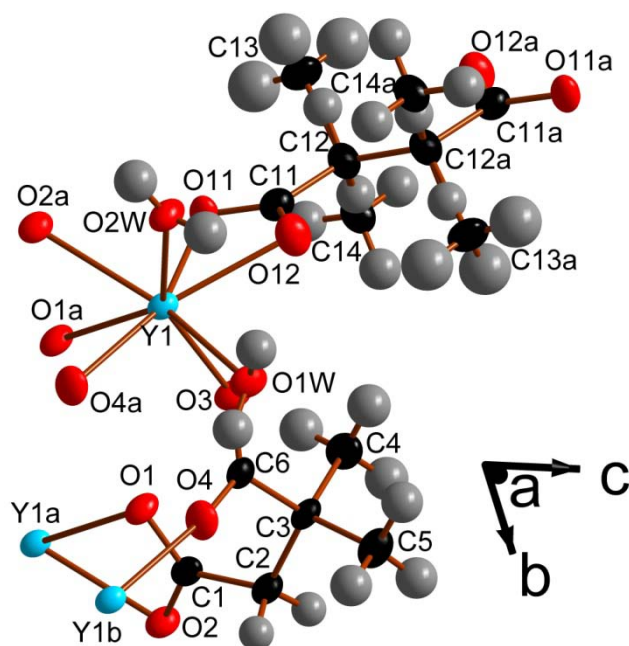


Fig. S16 The asymmetric unit of **7** with 40 % probability ellipsoids. The labels on the hydrogen atoms are omitted for the sake of clarity. Additional non-hydrogen atoms, included to illustrate the coordination sphere of all cations and oxygen atoms are labelled alphabetically. Both components of the disordered ligand are displayed and the colours are the same as in Fig. 5.

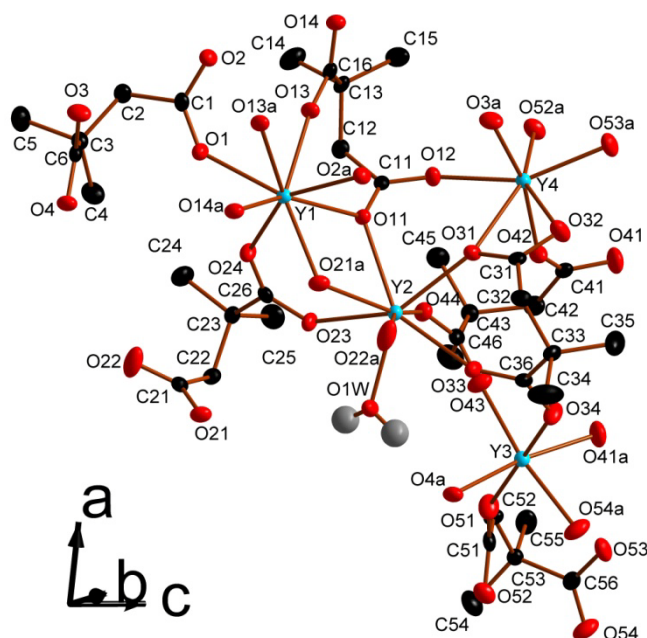


Fig. S17 The asymmetric unit of **8** with 40 % probability ellipsoids. The hydrogen atoms on the 2,2-DMS ligands are omitted for the sake of clarity. Additional non-hydrogen atoms, included to illustrate the coordination sphere of all cations, are labelled alphabetically and the colours are the same as Fig. 5.

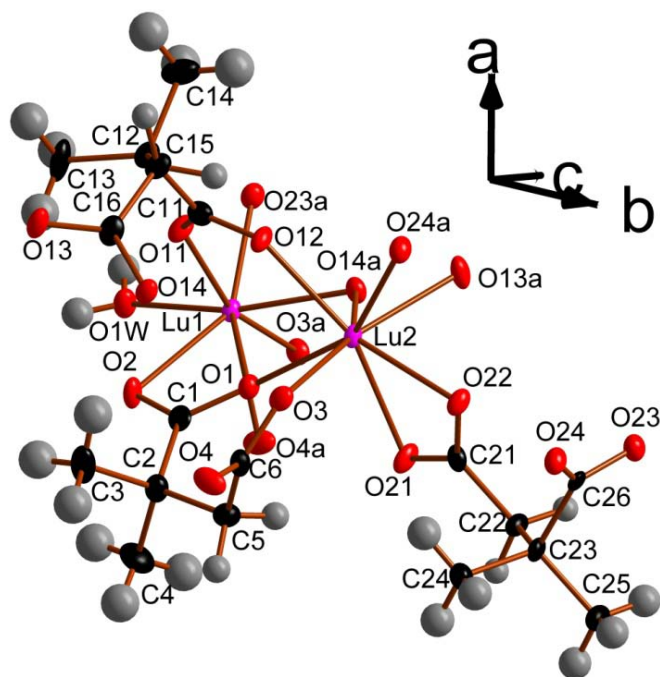


Fig. S18 The asymmetric unit of **10** with 60 % probability ellipsoids. Additional non-hydrogen atoms, included to illustrate the coordination sphere of all cations, are labelled alphabetically and the colours are the same as Fig. 8.

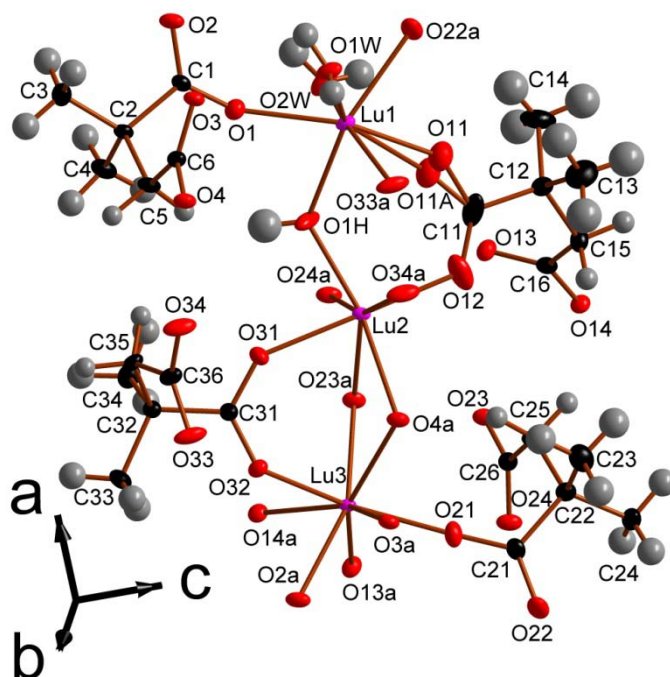


Fig. S19 The asymmetric unit of **11** with 60 % probability ellipsoids. Additional non-hydrogen atoms, included to illustrate the coordination sphere of all cations, are labelled alphabetically and the colours are the same as Fig. 8. Both positions of the disordered oxygen atoms, O11, are shown.

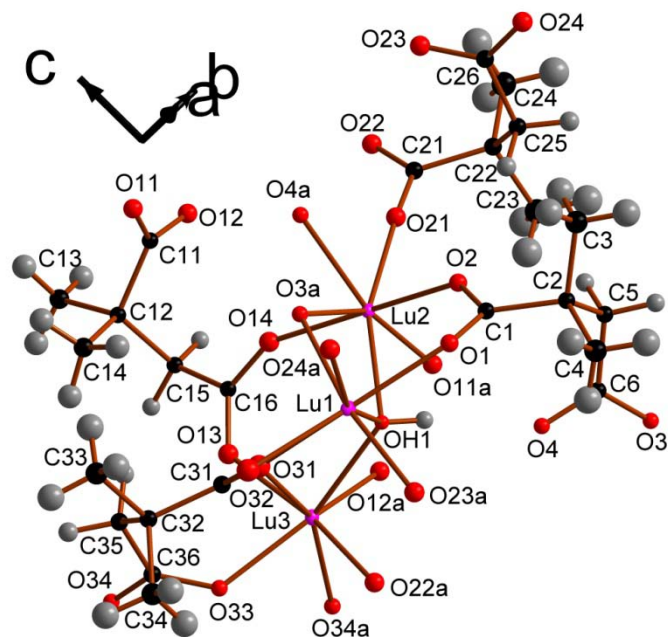


Fig. S20 The asymmetric unit of **12** with 40 % probability ellipsoids. Additional non-hydrogen atoms, included to illustrate the coordination sphere of all cations, are labelled alphabetically and the colours are the same as Fig. 8.

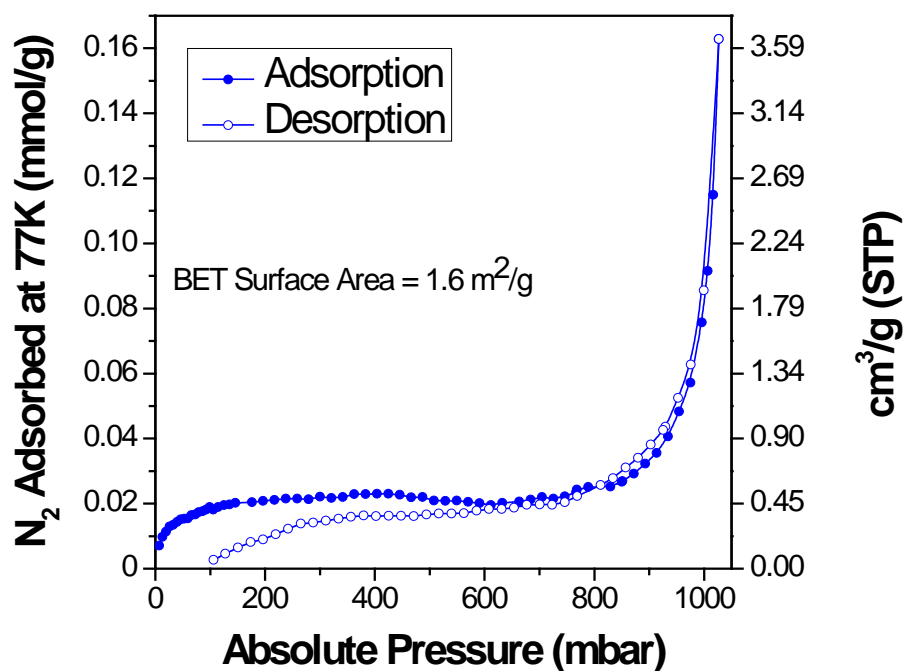


Fig. S21 Plot of Nitrogen sorption at 77 K versus pressure.

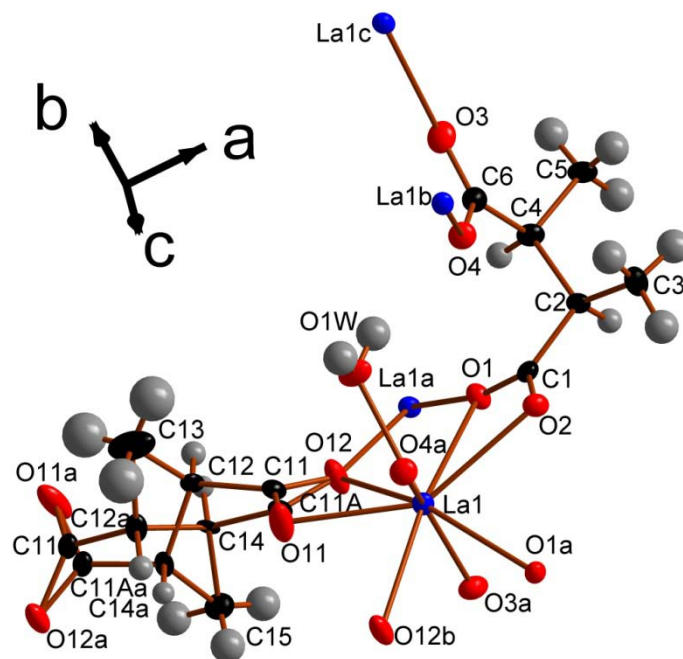


Fig. S22 The asymmetric unit of **13** with 60 % probability ellipsoids. Additional non-hydrogen atoms, used to illustrate the coordination sphere of all cations and ligand in the structure, are labelled alphabetically and the colours are the same as Fig. 1.

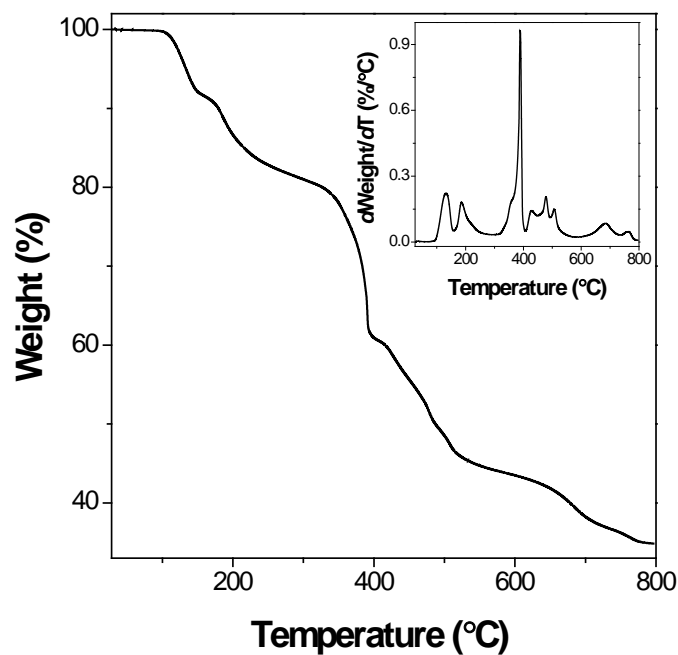


Fig. S23 Plot of weight loss versus temperature for **1** from TGA measurements. The insert shows the plot of the first derivative versus temperature highlighting the distinct periods of weight loss.

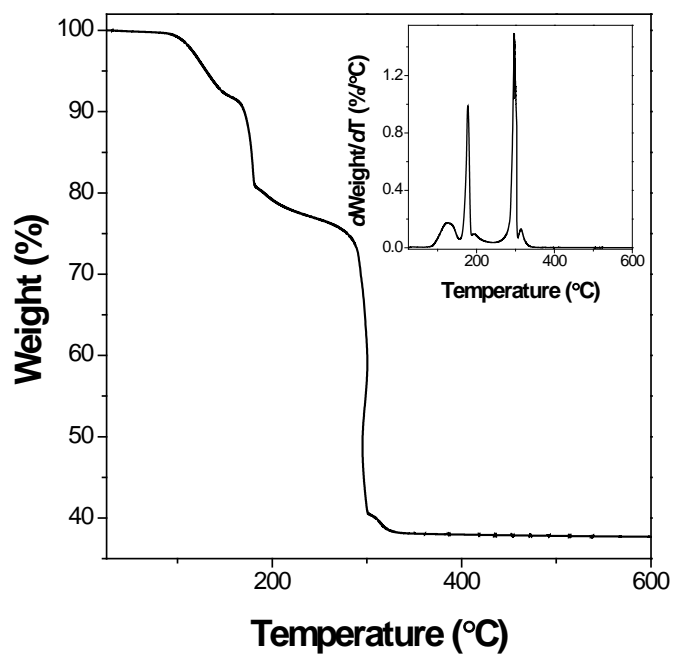


Fig. S24 Plot of weight loss versus temperature for **2** from TGA measurements. The insert shows the plot of the first derivative versus temperature.

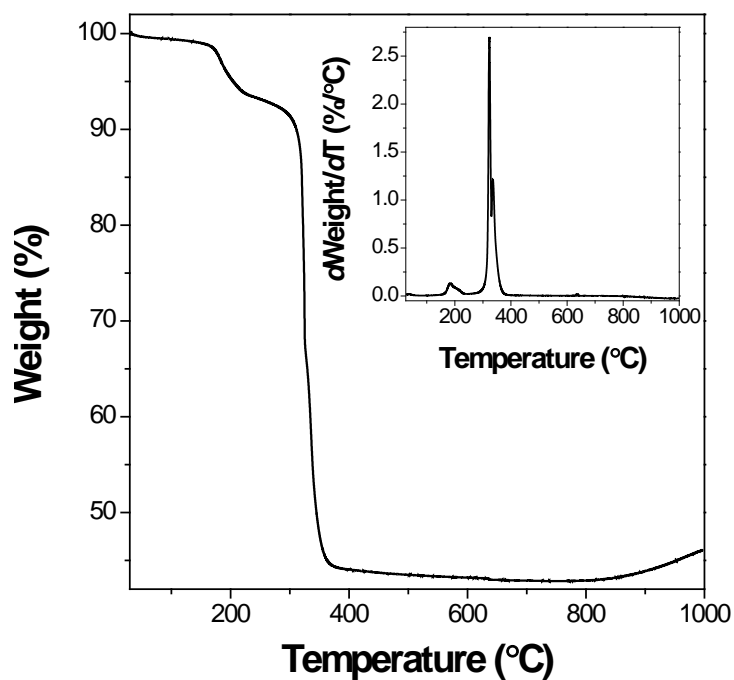


Fig. S25 Plot of weight loss versus temperature for **3** from TGA measurements. The insert shows the plot of the first derivative versus temperature.

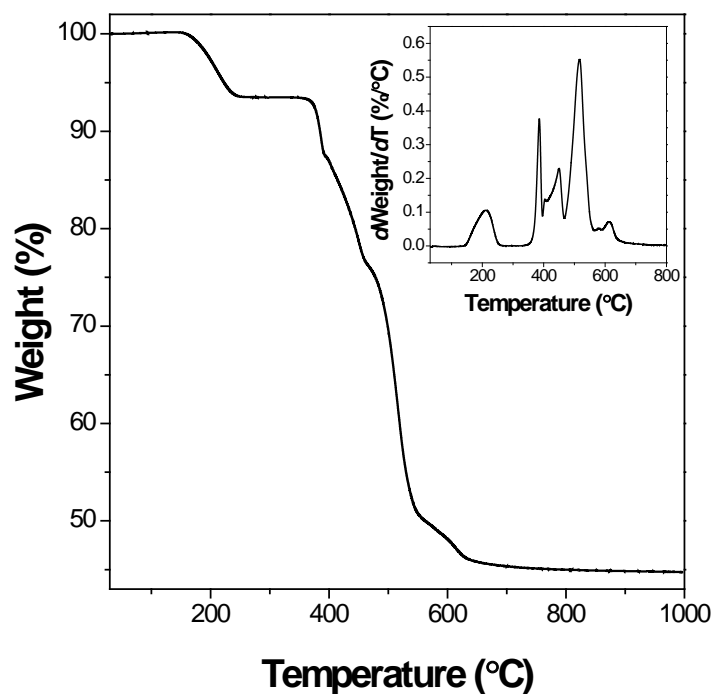


Fig. S26 Plot of weight loss versus temperature for **4** from TGA measurements. The insert shows the plot of the first derivative versus temperature.

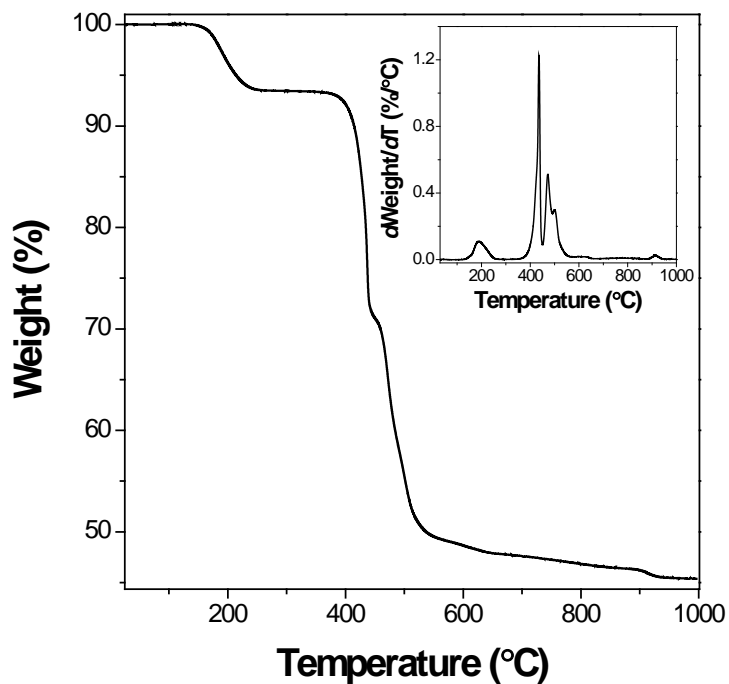


Fig. S27 Plot of weight loss versus temperature for **5** from TGA measurements. The insert shows the plot of the first derivative versus temperature.

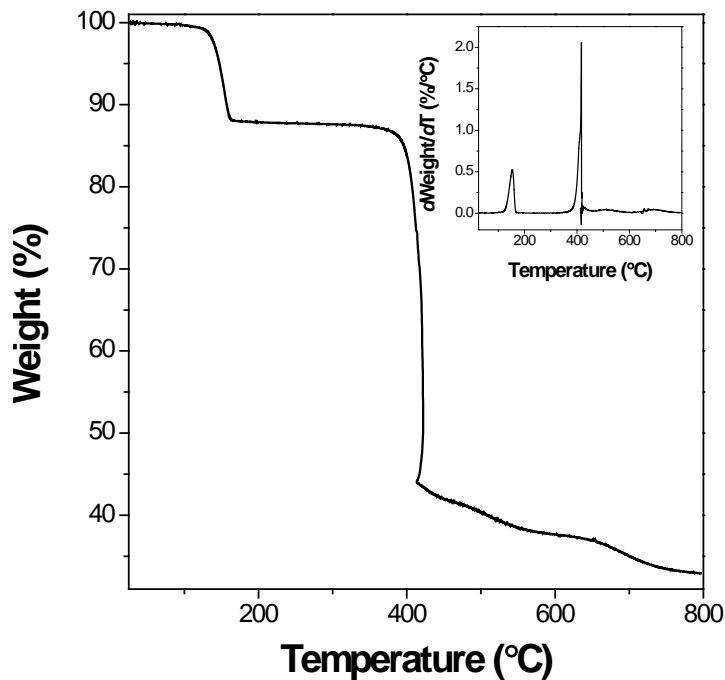


Fig. S28 Plot of weight loss versus temperature for **6** from TGA measurements. The insert shows the plot of the first derivative versus temperature.

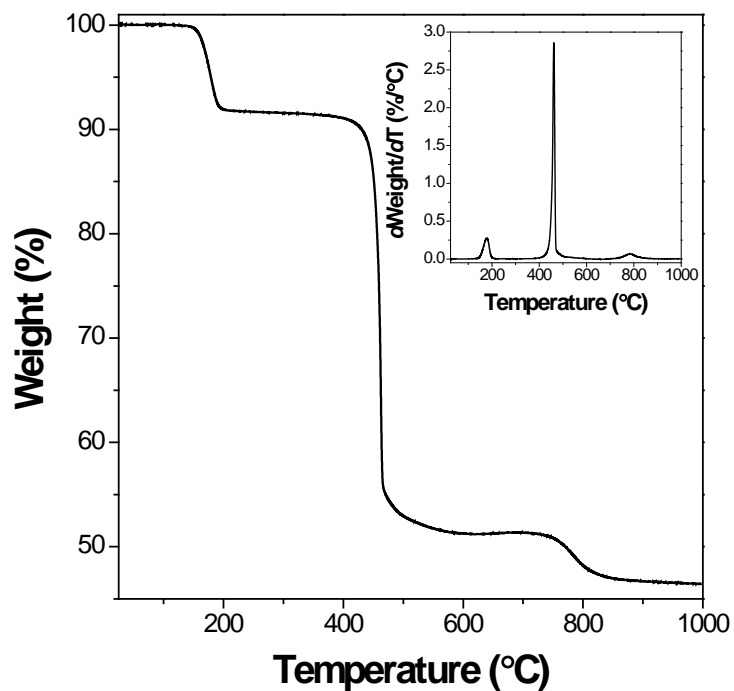


Fig. S29 Plot of weight loss versus temperature for **9** from TGA measurements. The insert shows the plot of the first derivative versus temperature.

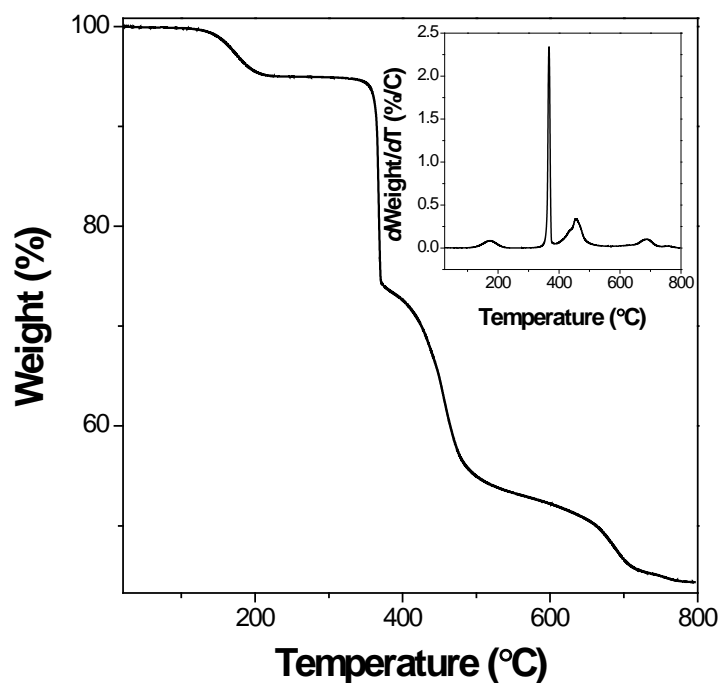


Fig. S30 Plot of weight loss versus temperature for **13** from TGA measurements. The insert shows the plot of the first derivative versus temperature.

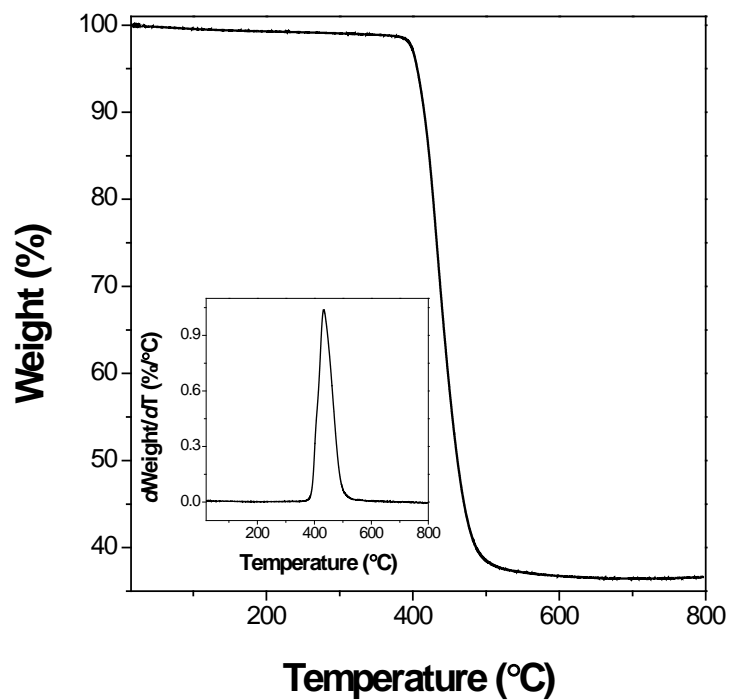


Fig. S31 Plot of weight loss versus temperature for **14** from TGA measurements. The insert shows the plot of the first derivative versus temperature.

1. *CrysAlis PRO*; Version 171.35.21, Agilent Technologies, Yarnton, Oxfordshire, England, 2012.
2. P. T. Beurskens, G. Beurskens, R. de Gelder, S. Garcia-Granda, R. O. Gould and J. M. M. Smits, *The DIRDIF2008 program system*, Crystallography Laboratory, University of Nijmegen, Nijmegen, The Netherlands, 2008.
3. G. M. Sheldrick, *Acta Crystallogr.*, 2008, **A64**, 112-122.
4. L. J. Farrugia, *A Windows Program for Crystal Structure Analysis*, University of Glasgow, Glasgow, UK, 1998.
5. a) K. D. Dobson and A. J. McQuillan, *Spectrochim. Acta Part A*, 1999, **55**, 1395-1405; b) C. Livage, C. Egger and G. Férey, *Chem. Mater.*, 2001, **13**, 410-414.
6. B. A. Hunter and C. J. Howard, *A computer program for Rietveld analysis of X-ray and neutron powder diffraction patterns*, Lucas Heights Laboratories, Lucas Heights, Australia, 1998.